sensors

MDPI

Article

Impact of Chamber/Annealing Temperature on the Endurance Characteristic of Zr:HfO_2 Ferroelectric Capacitor

Yejoo Choi [1], Changwoo Han [1], Jaemin Shin [2], Seungjun Moon [1], Jinhong Min [3], Hyeonjung Park [1], Deokjoon Eom [4], Jehoon Lee [4] and Changhwan Shin [5,*]

[1] Department of Electrical and Computer Engineering, Sungkyunkwan University, Suwon 16419, Korea; mirmail9206@skku.edu (Y.C.); cwhan0105@g.skku.edu (C.H.); scott93@skku.edu (S.M.); hyun7256@g.skku.edu (H.P.)
[2] Department of Electrical Engineering, University of Notre Dame, Notre Dame, IN 46556, USA; jshin6@nd.edu
[3] Department of Materials Science and Engineering, University of Michigan, Ann Arbor, MI 48109, USA; jinhongm@umich.edu
[4] School of Advanced Materials Sciences and Engineering, Sungkyunkwan University, Suwon 16419, Korea; vish0316@skku.edu (D.E.); iryes4832@skku.edu (J.L.)
[5] School of Electrical Engineering, Korea University, Seoul 02841, Korea
* Correspondence: cshin@korea.ac.kr

Abstract: The endurance characteristic of Zr-doped HfO_2 (HZO)-based metal–ferroelectric–metal (MFM) capacitors fabricated under various deposition/annealing temperatures in the atomic layer deposition (ALD) process was investigated. The chamber temperature in the ALD process was set to 120 °C, 200 °C, or 250 °C, and the annealing temperature was set to 400 °C, 500 °C, 600 °C, or 700 °C. For the given annealing temperature of 700 °C, the remnant polarization ($2P_r$) was 17.21 μC/cm^2, 26.37 μC/cm^2, and 31.8 μC/cm^2 at the chamber temperatures of 120 °C, 200 °C, and 250 °C, respectively. For the given/identical annealing temperature, the largest remnant polarization (P_r) was achieved when using the chamber temperature of 250 °C. At a higher annealing temperature, the grain size in the HZO layer becomes smaller, and thereby, it enables to boost up P_r. It was observed that the endurance characteristics for the capacitors fabricated under various annealing/chamber temperatures were quite different. The different endurance characteristics are due to the oxygen and oxygen vacancies in ferroelectric films, which affects the wakeup/fatigue behaviors. However, in common, all the capacitors showed no breakdown for an externally applied pulse (up to 10^8 cycles of the pulse).

Keywords: ferroelectric capacitor; hafnium zirconium oxide; chamber temperature; polarization; endurance

Citation: Choi, Y.; Han, C.; Shin, J.; Moon, S.; Min, J.; Park, H.; Eom, D.; Lee, J.; Shin, C. Impact of Chamber/Annealing Temperature on the Endurance Characteristic of Zr:HfO_2 Ferroelectric Capacitor. *Sensors* **2022**, *22*, 4087. https://doi.org/10.3390/s22114087

Academic Editor: Toshikazu Nishida

Received: 13 April 2022
Accepted: 24 May 2022
Published: 27 May 2022

1. Introduction

Ferroelectric materials have been widely used/adopted for various types of sensors and devices. Among various ferroelectric materials, HfO_2-based ferroelectric devices have attracted great interest [1]. A HfO_2-based ferroelectric film with fluorite structure solved the drawbacks in the conventional perovskite–structure ferroelectrics. They have extraordinary compatibility with complementary metal-oxide semiconductors (CMOS) and excellent ferroelectricity at ultra-thin (<10 nm) thickness [2,3]. The ferroelectric properties of HfO_2-based film originated from the non-centrosymmetric orthorhombic phase (o-phase), and the stabilization of the o-phase enhances the ferroelectric behavior [4]. The ferroelectric phase can be stabilized through annealing, and it can be characterized differently by various factors, such as dopant, thickness of ferroelectric film, and deposition temperature [5,6].

Various dopants with HfO_2 have been studied, and among them, zirconium (Zr) was chosen as the most promising material for memory and logic devices [6,7]. Unlike other dopants remaining stable at much lower concentration, Zr dopants can be stable with the

same percentage as Hf in HZO film. Moreover, ferroelectric properties using Zr dopants can be obtained in much lower annealing temperature (T_A) than other dopants.

As a memory device, the ferroelectric films require good endurance properties. The main factor affecting the endurance is the oxygen vacancy (V_O) in ferroelectric films. During the electric field cycling, V_O is redistributed, which results in the uniform distribution of V_O in the bulk region of the ferroelectric layer [8]. This phenomenon increases the P_r value by decreasing the built-in field and then decreases the P_r value with additional cycling. This increase in P_r is called the "wake-up effect" and the decrease in P_r is called the "fatigue effect" [9,10]. The breakdown of the films is observed when V_O forms a filament, which results as a leakage path. Therefore, it is very important to control the amount of V_O for the reliability of memory devices.

The characteristics of ferroelectric films can vary through various methods such as adjusting the doping effect and the chamber temperature during ALD [11,12]. Adjusting the temperature of the chamber during ALD changes the deposition rate and the average grain size of the film [6,13]. These factors change the distribution of V_O, which can significantly affect the ferroelectricity and the endurance properties. However, studies on the relationship of the effects of chamber temperature and the endurance performance are still lacking.

In this study, the ferroelectric properties of TiN/HZO/TiN capacitors with different chamber temperatures were investigated. The electrical characteristics of each capacitor were analyzed through polarization–voltage (P-V) curves and leakage current–voltage (I-V) curves. Moreover, the endurance performance related to the amount of V_O was investigated under different chamber temperatures.

2. Fabrication

The illustrated cross-sectional view and fabrication flow of TiN/HZO/TiN capacitors are shown in Figure 1a,b, respectively. First, a p^+-doped silicon wafer was cleaned by a SPM cleaning, which was followed by the conventional RCA method (i.e., SC-1 cleaning and SC-2 cleaning). Then, the 50 nm-thick TiN bottom electrode was deposited on the Si substrate by using DC sputtering. The 10 nm-thick HZO thin film was deposited by thermal atomic layer deposition (ALD). The tetrakis (ethylmethylamino) hafnium (TEMAH), tetrakis (ethylmethylamino) zirconium (TEMAZ), and H_2O source precursor were used for the ALD process to deposit the HZO film. The Hf and Zr was deposited using an ALD supercycle [14]. The aforementioned fabrication was identically completed but at three different chamber temperatures (T_{CH}) of 120 °C, 200 °C, and 250 °C. As shown in Figure 1c, the growth per (super)cycle of HZO film decreased as the chamber temperature (T_{CH}) increased. The total number of supercycles to make 10 nm-thick HZO thin film was set to 56, 61, and 68 for T_{CH} of 120 °C, 200 °C, and 250 °C, respectively. The 50 nm-thick TiN top electrode on the HZO layer was deposited using the DC sputtering used for bottom electrodes. Then, the HZO capacitors were patterned to have the electrode area of 6400 μm^2. Finally, the post-metallization annealing (PMA) was completed by rapid thermal annealing (RTA) at 400, 500, 600, and 700 °C for 30 s in N_2 atmosphere to crystallize the HZO films.

To investigate the electrical characteristics of HZO capacitors, P-V curves and I-V curves were measured using semiconductor parameter analyzer (Keithley 4200-SCS). The X-ray photoelectron spectroscopy (XPS), transmission electron microscopy (TEM), and energy-dispersive X-ray spectroscopy (EDS) were used to characterize the HZO capacitor.

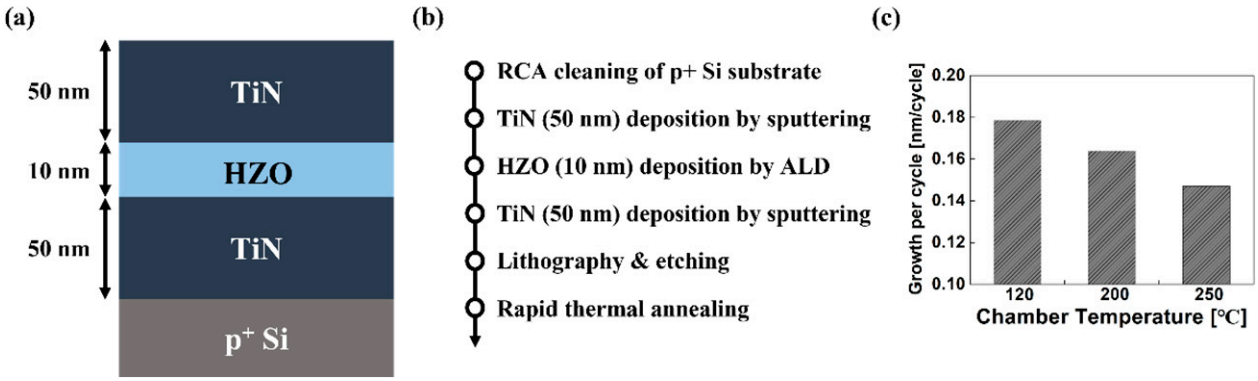

Figure 1. (**a**) Illustrated cross-sectional view of the fabricated TiN/HZO/TiN capacitor, and (**b**) its fabrication process flow. The HZO layer were deposited under three different temperatures in chamber, i.e., 120 °C, 200 °C, and 250 °C. (**c**) Growth per cycle of HZO film for three different chamber temperatures. Note that the growth per cycle is decreased with increasing the chamber temperature, which is due primarily to the decreasing contribution of surface exchange reaction [13].

3. Results and Discussion

3.1. Electrical Characteristics

Figure 2a–c show the measured P-V curves of the TiN/HZO/TiN capacitors with a few annealing temperatures (i.e., 400, 500, 600, and 700 °C) at T_{CH} of 120 °C, 200 °C, and 250 °C, respectively. The measured P_r was increased at a higher T_A for all the capacitors. This is mainly because the ratio of o-phase in the HZO layer was increased at the higher T_A [2,10]. For a given T_A, a higher P_r was implemented at a higher T_{CH}. This achievement was physically originated from a few reasons, as follows: (1) The number of supercycles increases at a higher T_{CH} because the deposition rate of HZO film is decreased at a higher T_{CH} (see Figure 1c). This leads to increasing the number of HfO_2/ZrO_2 nanolaminates, resulting in the improved P_r [15]. (2) The average grain size of HZO film becomes smaller at a higher deposition temperature, if H_2O is used as the oxygen source in ALD [13]. The smaller average grain size enables us to boost up the ferroelectric polarization [10,16]. This is primarily originated from the tetragonal phase (t-phase) and the orthorhombic phase (o-phase), which are easily stabilized in smaller grain regions. (3) Because defects (noted as V_O) are likely to be accumulated along the grain boundaries, the smaller grain size is likely to build more grain boundaries for a given volume. This would distort the distribution of V_O. Herein, it is noteworthy that the well-balanced distribution of V_O in HZO films should help stabilize the ferroelectric phase, and thereby, the ferroelectric polarization would be enhanced [10,17].

In Figure 2d, the leakage current of TiN/HZO/TiN capacitors fabricated at different T_A and T_{CH} was measured. It turned out that for a given T_{CH} (T_A), the leakage current increases at a higher T_A (T_{CH}). In the MFM ferroelectric capacitor, the leakage current is mostly originated from V_O (i.e., the higher V_O is, the more the leakage current flows [15]). In Section 3.2, with TEM, XPS, and EDS data, it is investigated how V_O is varied at different T_{CH}.

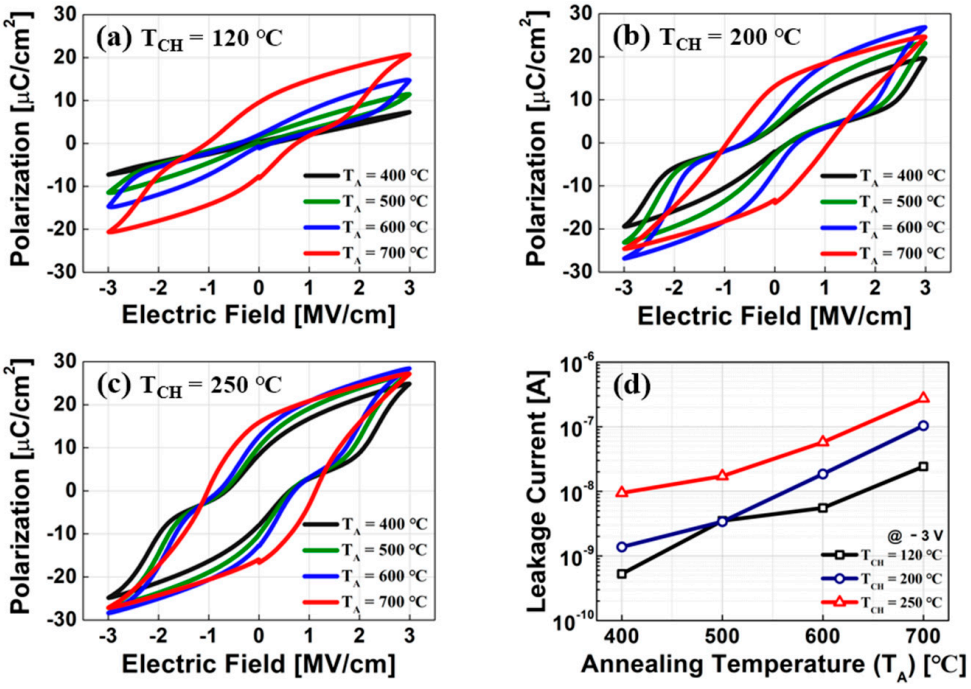

Figure 2. Measured polarization vs. electric field of TiN/HZO/TiN capacitor in which the HZO layer was deposited at the chamber temperature of (**a**) 120 °C, (**b**) 200 °C, and (**c**) 250 °C. Note that four different annealing temperatures (T_A = 400~700 °C) were used for better implementing the ferroelectric characteristics of the HZO layer. (**d**) Measured leakage current-vs.-annealing temperature for three different chamber temperatures. Note that the leakage current was measured with the voltage of −3 V across the ferroelectric capacitor.

3.2. XPS, TEM, and EDS

Figure 3 shows the XPS depth profile of the TiN/HZO/TiN capacitor at T_A of 700 °C under three different T_{CH} values. The atomic percent clearly reveals the TiN/HZO/TiN device structure. Among many atoms in the profile, the O 1s in the HZO layer is deconvoluted to figure out the oxygen bonds in great detail (see Figure 4). Notice that the intensities of each net peak were normalized to the same scale. The O 1s was divided into two peaks (i.e., lattice oxygen peak and sub-oxide peak). The lattice oxygen peak describes the bonds such as Hf-O and Zr-O, of which the binding energy is located in ≈532 eV. The sub-oxide peak indicates oxygen in a lattice, which does not contain its full complement of oxygen (and therefore, indicating the presence of vacancies). The peak describes the bonds such as oxygen interstitial and oxygen vacancy (V_O), of which the binding energy locates at ≈534 eV.

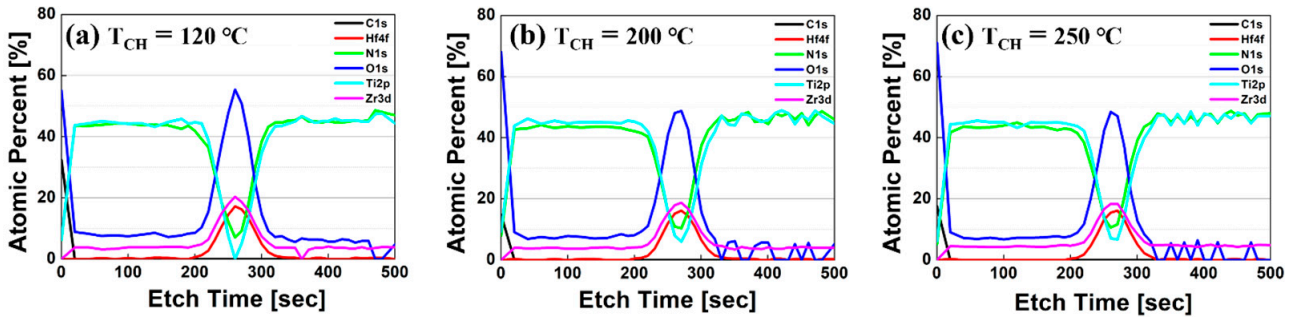

Figure 3. Measured XPS depth profiles of TiN (50 nm)/HZO (10 nm)/TiN (50nm) capacitor, which was fabricated at three different chamber temperatures: (**a**) 120 °C, (**b**) 200 °C, and (**c**) 250 °C.

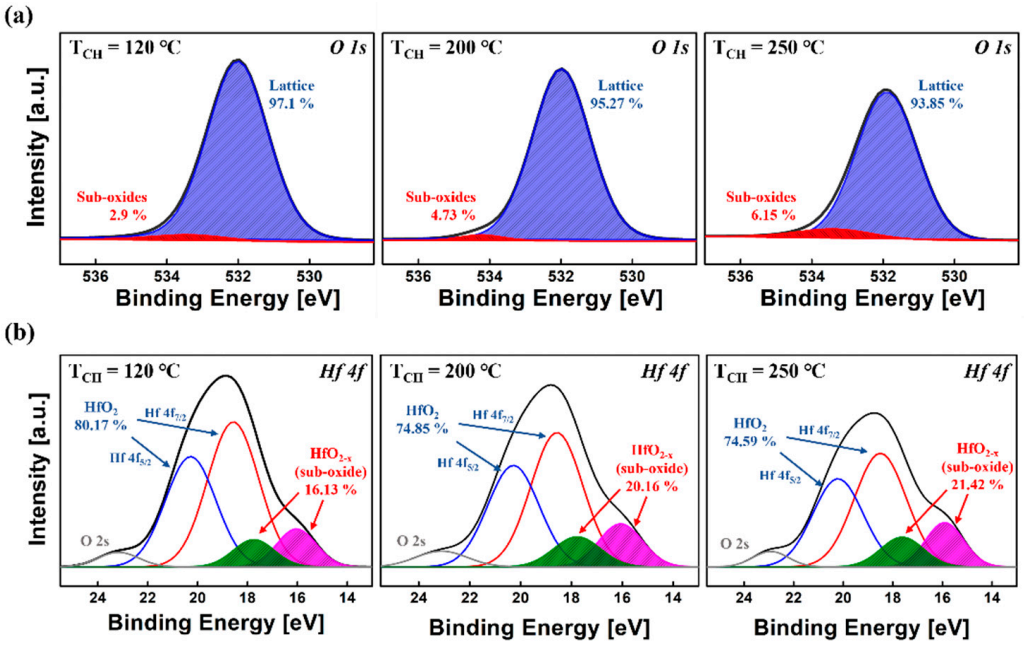

Figure 4. Measured (**a**) XPS O 1s spectra and (**b**) XPS Hf 4f spectra of the HZO film in TiN/HZO/TiN capacitor, which was fabricated at three different chamber temperatures (i.e., 120 °C, 200 °C and 250 °C). The O 1s levels were deconvoluted into two peaks, i.e., lattice oxygen peak and sub-oxide peak. The Hf 4f levels were deconvoluted into five peaks, i.e., HfO_2 peaks, sub-oxide peaks, and O 2s peak. Each intensity level was normalized to the same scale.

The amount of O 1s in Figures 3 and 4a confirms that there was a difference in the ratio of O 1s in HZO film, depending on three different T_{CH}. The intensity of peak amplitude is decreased at a higher T_{CH}. In addition, the atomic percent of Ti and N is decreased at a lower T_{CH} (see Figure 3). In other words, the formation of the dead layer (i.e., TiO_2 and TiON) between the HZO layer and the TiN electrode was suppressed at a lower T_{CH}, which reduces the amount of V_O in the HZO layer. It was confirmed that the ratio of V_O increases if the dead layer between the HZO layer and the TiN electrode is formed [18].

It was observed that the percentage of sub-oxide bonding is increased at a higher T_{CH} (see Figure 4a). This also indicates that the ratio of V_O increases. In other words, the oxygen should move from the HZO layer to the electrodes to make the interfacial layer, and thereby, the V_O in HZO film is increased [17]. Hence, the increased V_O means that the larger amount of oxygen has moved toward the interfacial layer. In addition, in the XPS for Hf 4f spectra, it was confirmed that the sub-oxide means the oxygen vacancy in the HZO layer [19]. As shown in Figure 4b, it was observed that the ratio of sub-oxide in Hf 4f spectra is increased when T_{CH} is increased, which leads to a higher V_O. In summary, the ratio of oxygen in the HZO layer becomes smaller at a higher T_{CH}, which is closely associate with the amount of V_O. A higher T_{CH} would make the ratio of V_O higher. This is well agreed to the increase in leakage current at a higher T_{CH} because of the increased V_O (see Figure 2d).

Figure 5a–c show the TEM image of TiN/HZO/TiN capacitors fabricated at three different chamber temperatures (T_{CH}) with T_A of 500 °C. It was observed that the thicknesses of the HZO films were all the same: 10 nm. Figure 5d shows the EDS image of the TiN/HZO/TiN capacitor fabricated with T_A of 700 °C. The ratio of elements in each layer can be determined through the EDS analysis (see Table 1). For example, the largest (smallest) atomic rate of oxygen in HZO films was implemented with T_{CH} of 120 °C (250 °C), which was consistent with the XPS analysis. The amount of oxygen vacancy (V_O) was increased, as the oxygen was decreased with increasing T_{CH}. However, the discrepancy of the ratio of elements exists between the XPS and EDS analysis. Note that the purpose of the EDS analysis in this work was to confirm/verify the change of oxygen atoms.

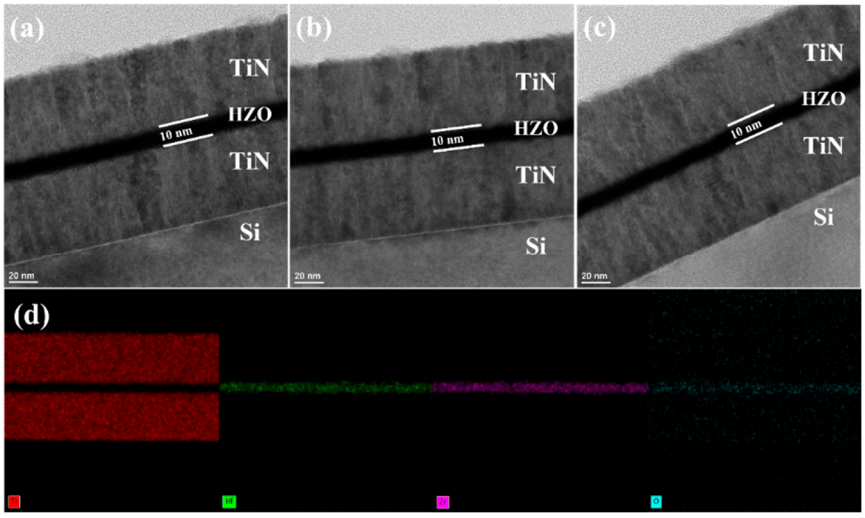

Figure 5. The transmission electron microscopy (TEM) image of the TiN/HZO/TiN capacitor, which was fabricated at three different chamber temperatures: (**a**) 120 °C, (**b**) 200 °C, and (**c**) 250 °C. (**d**) The energy-dispersive spectroscopy (EDS) images for titanium, hafnium, zirconium, and oxygen in the HZO capacitor at the chamber temperature of 250 °C.

Table 1. Energy-dispersive spectrometer (EDS) quantification of elements in HZO layer.

Chamber Temperature (T_{CH}) (°C)	Atomic Percent (%)					
	Ti	N	Hf	Zr	O	Si
120	4.50	9.76	20.90	18.16	30.44	16.24
200	9.20	4.49	24.95	21.00	23.32	17.03
250	10.74	10.80	24.75	21.18	19.38	13.15

3.3. Endurance

The endurance (especially, affected by an electric field cycling) in TiN/HZO/TiN capacitors was investigated. Figure 6 shows the pulsing scheme for evaluating the endurance of the capacitors. The electric field cycling was completed with using a trapezoidal pulse, and the number of cycling was applied up to 10^8. After the cycling pulses were applied, a triangular pulse was applied to measure the P-V characteristic of the capacitor. Note that both pulses have the same peak amplitude of 3 V. The P-V characteristic of each capacitor was compared to each other (see Figure 7).

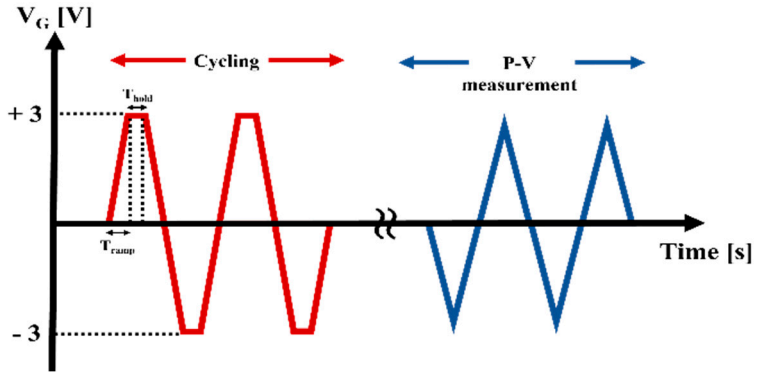

Figure 6. Illustrated pulsing scheme for analyzing the wake−up and fatigue behaviors of TiN/HZO/TiN capacitor. The cycling was first completed using the trapezoidal pulse with the ramp time (T_{ramp}) of 1 μs and the hold time (T_{hold}) of 1 μs. Afterwards, the P-V measurement was made using the triangular pulse. Note that the amplitude for both pulses is set to 3 V.

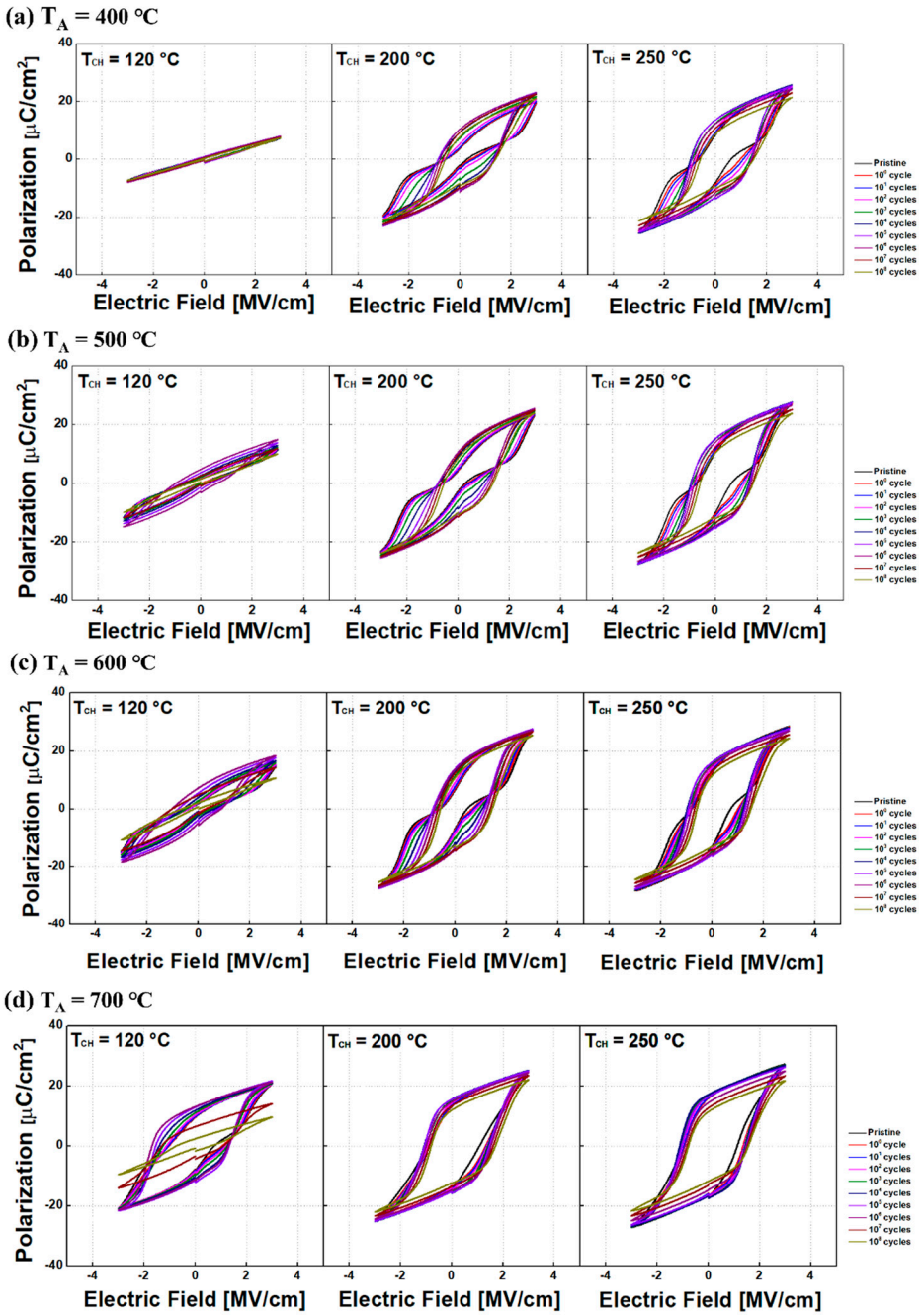

Figure 7. Measured polarization vs. electric field (PE) characteristics of TiN/HZO/TiN capacitors fabricated at various chamber temperatures (i.e., 120 °C, 200 °C, and 250 °C) as well as at various annealing temperatures (T_A): (**a**) 400 °C, (**b**) 500 °C, (**c**) 600 °C, and (**d**) 700 °C. Note that the different numbers of cycles were used to explore the endurance characteristics of the ferroelectric capacitor.

The remnant polarization (P_r) of each HZO capacitor in pristine state is as follows: In case of T_{CH} of 120 °C, P_r of 0.28 μC/cm^2, 1.17 μC/cm^2, 2.68 μC/cm^2, and 17.21 μC/cm^2 was observed for T_A of 400 °C, 500 °C, 600 °C, and 700 °C, respectively. In case of T_{CH} of 200 °C, P_r of 5.66 μC/cm^2, 6.88 μC/cm^2, 13.43 μC/cm^2, and 26.37 μC/cm^2 was observed for T_A of 400 °C, 500 °C, 600 °C, and 700 °C, respectively. Finally, in case of T_{CH} of 250 °C, P_r of 16.38 μC/cm^2, 20.46 μC/cm^2, 25.3 μC/cm^2, and 31.8 μC/cm^2 was observed for T_A of 400 °C, 500 °C, 600 °C, and 700 °C, respectively. Regardless of T_{CH}, it turned out that P_r was increased with increasing T_A. For a given/identical T_A, P_r can be improved with

higher T_{CH}. This is primarily because the amount of ferroelectric phase was increased with increasing either T_A or T_{CH} [2,9].

As shown in Figure 8, all the capacitors did not show any breakdown up to 10^8 cycles. However, depending on T_{CH}, the number of cycles at which the fatigue begins (i.e., P_r is about to decrease) is varied. Regardless of T_{CH}, higher P_r was observed with higher T_A. This is primarily originated from a well-distributed V_O in bulk region of HZO film at a higher T_A [10].

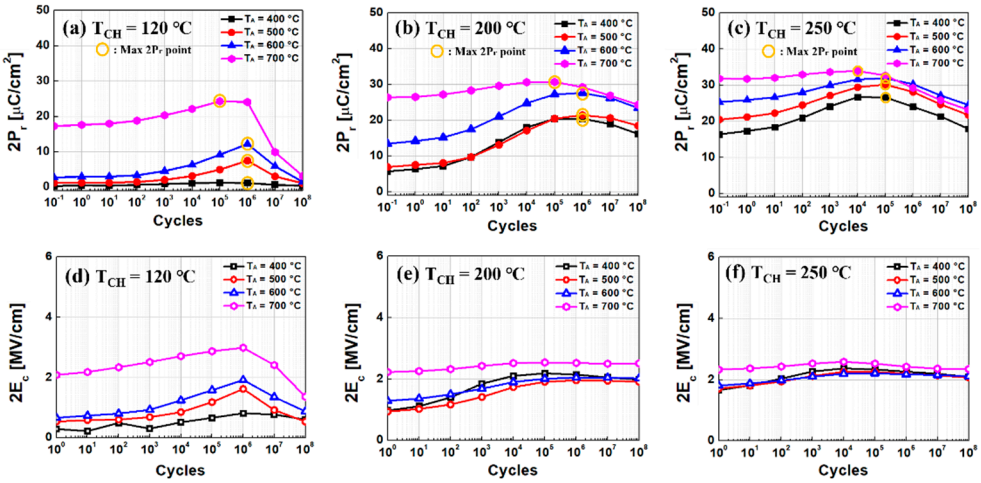

Figure 8. Measured representative ferroelectric characteristics (i.e., remnant polarization ($2P_r$) and/or coercive electric field ($2E_c$)) versus cycles, for given three different chamber temperatures, (**a**,**d**) 120 °C, (**b**,**e**) 200 °C, and (**c**,**f**) 250 °C with four different annealing temperatures (T_A from 400 °C to 700 °C). The yellow−colored circle indicates the max point of $2P_r$.

It is known that the ferroelectric characteristics (notably, represented by P_r) can be improved as the number of cycles increases (a.k.a., wake-up effect). However, the ferroelectric characteristics should not be ever enhanced because of fatigue. The maximum value of $2P_r$ and the number of cycles at which fatigue begins (a.k.a. critical number of cycles) are summarized in Figure 9. It turned out that the value of $2P_r$ increases with increasing T_A. (However, only for T_{CH} of 120 °C, T_A of 400 °C shows insufficient ferroelectricity, which results in a low $2P_r$.) Compared to the other T_{CH} of 200 °C and 250 °C, the measured P_r was significantly degraded for T_{CH} of 120 °C. When H_2O reactant is used as an oxygen source in ALD, the lowest T_{CH} (i.e., 120 °C) forms the largest average grain size. This causes more formation of monoclinic phase (m-phase), which is non-ferroelectric phase, and it makes the depolarization field stronger [20,21]. Therefore, for T_{CH} of 120 °C, the sudden decrease in P_r in the HZO capacitor was understood with less m-phase.

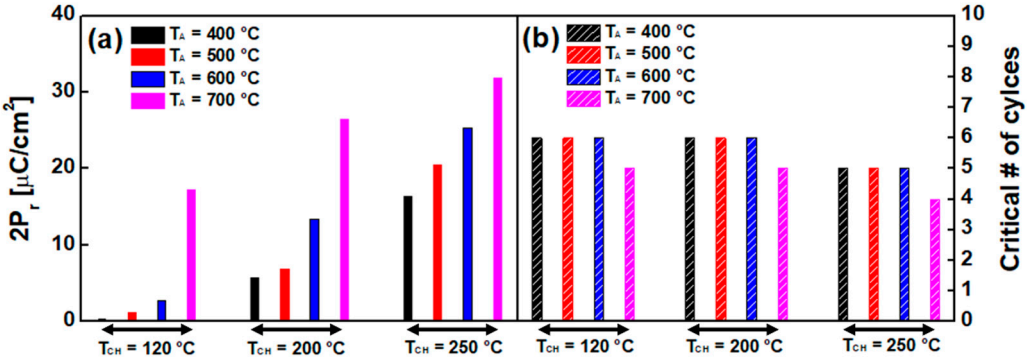

Figure 9. (**a**) Maximum remnant polarization ($2P_r$) and (**b**) critical number of cycles at which fatigue begins for given three different chamber temperatures, 120 °C, 200 °C, and 250 °C, with four different annealing temperatures (T_A from 400 °C to 700 °C).

In Figure 9, it was also observed that the critical number of cycles (i.e., the number of cycles at which fatigue begins) decreases at a higher T_{CH} for the same T_A. As shown in Figures 2d and 4, more V_O in the ferroelectric layer was observed at a higher T_{CH}, and thereby, so is the leakage current in HZO capacitor (this is because the excessive amount of V_O makes undesirable conducting paths in the HZO film [10,22]). The more V_O in the ferroelectric film should cause the ferroelectricity of the film to be fatigued at a rapid pace.

4. Conclusions

In this work, the impact of chamber/annealing temperatures in the atomic layer deposition (ALD) process on the ferroelectric property of the HZO layer in a TiN/HZO/TiN capacitor was investigated. Regardless of the chamber temperature (T_{CH}), a higher remnant polarization (P_r) was achieved with a higher annealing temperature (T_A). For a given T_A, P_r was increased with increasing T_{CH}. This ferroelectricity was well retained up to the cycles of 10^8. However, the capacitors fabricated under the three different T_{CH} showed different endurance performances in terms of the critical number of cycles. This is due primarily to the oxygen and oxygen vacancies in the HZO layer (which was quantitatively analyzed and confirmed by XPS and EDS analysis). The more oxygen vacancies (V_O) at a higher T_{CH} enabled for P_r to be improved, but they made an undesirable conducting path in the HZO film, resulting in decreasing the critical number of cycles.

Author Contributions: Conceptualization, Y.C., J.S., S.M. and C.S.; Data curation, Y.C., C.H., J.S., S.M., J.M. and C.S.; Formal analysis, Y.C., C.H., S.M., H.P. and C.S.; Funding acquisition, C.S.; Investigation, Y.C., J.S., S.M. and J.M.; Methodology, Y.C., C.H., J.S., S.M., J.M., D.E. and J.L.; Project administration, C.S.; Resources, Y.C.; Supervision, C.S.; Validation, Y.C., J.S., S.M., J.M. and C.S.; Visualization, Y.C., C.H., J.S. and C.S.; Writing—Original draft, Y.C. and C.S.; Writing—Review and editing, C.S., Y.C., C.H., J.S., S.M. and J.M. equally contributed to this work. All authors have read and agreed to the published version of the manuscript.

Funding: This work was funded by a National Research Foundation of Korea (NRF) grant funded by the Korean government (MSIP) (No. 2020R1A2C1009063, 2020M3F3A2A01082326, 2020M3F3A2A0108-1672 and 2020M3F3A2A02082436).

Institutional Review Board Statement: Not applicable.

Informed Consent Statement: Not applicable.

Data Availability Statement: The data presented in this study are available on request from the corresponding author.

Conflicts of Interest: The authors declare no conflict of interest.

References

1. Du, J.; Xie, D.; Zhang, Q.; Zhong, H.; Meng, F.; Fu, X.; Sun, Q.; Ni, H.; Li, T.; Guo, E.-J.; et al. A robust neuromorphic vision sensor with optical control of ferroelectric switching. *Nano Energy* **2021**, *89*, 106439. [CrossRef]
2. Kim, H.J.; An, Y.; Jung, Y.C.; Mohan, J.; Yoo, J.G.; Kim, Y.I.; Hernandez-Arriaga, H.; Kim, H.S.; Kim, J.; Kim, S.J. Low-Thermal-Budget Fluorite-Structure Ferroelectrics for Future Electronic Device Applications. *Phys. Status Solidi (RRL) Rapid Res. Lett.* **2021**, *15*, 2100028. [CrossRef]
3. Fan, Z.; Chen, J.; Wang, J. Ferroelectric HfO2-based materials for next-generation ferroelectric memories. *J. Adv. Dielectr.* **2016**, *6*, 1630003. [CrossRef]
4. Kim, T.; An, M.; Jeon, S. Evolution of crystallographic structure and ferroelectricity of $Hf_{0.5}Zr_{0.5}O_2$ films with different deposition rate. *AIP Adv.* **2020**, *10*, 015104. [CrossRef]
5. Kim, K.D.; Park, M.H.; Kim, H.J.; Kim, Y.J.; Moon, T.; Lee, Y.H.; Hyun, S.D.; Gwon, T.; Hwang, C.S. Ferroelectricity in undoped-HfO_2 thin films induced by deposition temperature control during atomic layer deposition. *J. Mater. Chem. C* **2016**, *4*, 6864–6872. [CrossRef]
6. Park, M.H.; Lee, Y.H.; Kim, H.J.; Kim, Y.J.; Moon, T.; Kim, K.D.; Muller, J.; Kersch, A.; Schroeder, U.; Mikolajick, T.; et al. Ferroelectricity and antiferroelectricity of doped thin HfO2-based films. *Adv. Mater.* **2015**, *27*, 1811–1831. [CrossRef]
7. Alessandri, C.; Pandey, P.; Abusleme, A.; Seabaugh, A. Switching Dynamics of Ferroelectric Zr-Doped HfO2. *IEEE Electron Device Lett.* **2018**, *39*, 1780–1783. [CrossRef]

8. Zhou, Y.; Zhang, Y.K.; Yang, Q.; Jiang, J.; Fan, P.; Liao, M.; Zhou, Y.C. The effects of oxygen vacancies on ferroelectric phase transition of HfO2-based thin film from first-principle. *Comput. Mater. Sci.* **2019**, *167*, 143–150. [CrossRef]
9. Wang, C.; Qiao, H.; Kim, Y. Perspective on the switching behavior of HfO2-based ferroelectrics. *J. Appl. Phys.* **2021**, 129. [CrossRef]
10. Park, M.H.; Lee, Y.H.; Mikolajick, T.; Schroeder, U.; Hwang, C.S. Review and perspective on ferroelectric HfO2-based thin films for memory applications. *MRS Commun.* **2018**, *8*, 795–808. [CrossRef]
11. Alcala, R.; Richter, C.; Materano, M.; Lomenzo, P.D.; Zhou, C.; Jones, J.L.; Mikolajick, T.; Schroeder, U. Influence of oxygen source on the ferroelectric properties of ALD grown Hf1-xZrxO_2 films. *J. Phys. D Appl. Phys.* **2021**, *54*, 035102. [CrossRef]
12. Park, M.H.; Kim, H.J.; Kim, Y.J.; Lee, Y.H.; Moon, T.; Kim, K.D.; Hyun, S.D.; Fengler, F.; Schroeder, U.; Hwang, C.S. Effect of Zr Content on the Wake-Up Effect in Hf1-xZrxO2 Films. *ACS Appl. Mater. Interfaces* **2016**, *8*, 15466–15475. [CrossRef]
13. Lee, S.Y.; Kim, H.K.; Lee, J.H.; Yu, I.-H.; Lee, J.-H.; Hwang, C.S. Effects of O_3 and H_2O as oxygen sources on the atomic layer deposition of HfO2 gate dielectrics at different deposition temperatures. *J. Mater. Chem. C* **2014**, *2*, 2558–2568. [CrossRef]
14. Richey, N.E.; de Paula, C.; Bent, S.F. Understanding chemical and physical mechanisms in atomic layer deposition. *J. Chem. Phys.* **2020**, *152*, 040902. [CrossRef]
15. Kim, S.J.; Mohan, J.; Summerfelt, S.R.; Kim, J. Ferroelectric $Hf_{0.5}Zr_{0.5}O_2$ Thin Films: A Review of Recent Advances. *JOM* **2018**, *71*, 246–255. [CrossRef]
16. Kim, B.S.; Hyun, S.D.; Moon, T.; Do Kim, K.; Lee, Y.H.; Park, H.W.; Lee, Y.B.; Roh, J.; Kim, B.Y.; Kim, H.H.; et al. A Comparative Study on the Ferroelectric Performances in Atomic Layer Deposited $Hf_{0.5}Zr_{0.5}O_2$ Thin Films Using Tetrakis(ethylmethylamino) and Tetrakis(dimethylamino) Precursors. *Nanoscale Res. Lett.* **2020**, *15*, 72. [CrossRef]
17. Goh, Y.; Cho, S.H.; Park, S.K.; Jeon, S. Oxygen vacancy control as a strategy to achieve highly reliable hafnia ferroelectrics using oxide electrode. *Nanoscale* **2020**, *12*, 9024–9031. [CrossRef]
18. Chen, K.-Y.; Chen, P.-H.; Wu, Y.-H. Excellent reliability of ferroelectric HfZrOx free from wake-up and fatigue effects by NH3 plasma treatment. In Proceedings of the 2017 Symposium on VLSI Circuits, Kyoto, Japan, 5–8 June 2017.
19. Lee, Y.; Goh, Y.; Hwang, J.; Das, D.; Jeon, S. The Influence of Top and Bottom Metal Electrodes on Ferroelectricity of Hafnia. *IEEE Trans. Electron Devices* **2021**, *68*, 523–528. [CrossRef]
20. Mehmood, F.; Hoffmann, M.; Lomenzo, P.D.; Richter, C.; Materano, M.; Mikolajick, T.; Schroeder, U. Bulk Depolarization Fields as a Major Contributor to the Ferroelectric Reliability Performance in Lanthanum Doped $Hf_{0.5}Zr_{0.5}O_2$ Capacitors. *Adv. Mater. Interfaces* **2019**, *6*, 1901180. [CrossRef]
21. Chen, H.; Tang, L.; Liu, L.; Chen, Y.; Luo, H.; Yuan, X.; Zhang, D. Significant improvement of ferroelectricity and reliability in $Hf_{0.5}Zr_{0.5}O_2$ films by inserting an ultrathin Al_2O_3 buffer layer. *Appl. Surf. Sci.* **2021**, *542*, 148737. [CrossRef]
22. Mittmann, T.; Materano, M.; Chang, S.C.; Karpov, I.; Mikolajick, T.; Schroeder, U. Impact of Oxygen Vacancy Content in Ferroelectric HZO films on the Device Performance. In Proceedings of the 2020 IEEE International Electron Devices Meeting (IEDM), San Francisco, CA, USA, 12–18 December 2020; pp. 18.14.11–18.14.14.